

Dendritic flux avalanches in rectangular superconducting films – numerical simulations

J. I. Vestgård and Y. M. Galperin

Department of Physics, University of Oslo, P. O. Box 1048 Blindern, 0316 Oslo, Norway

T. H. Johansen

Department of Physics, University of Oslo, P. O. Box 1048 Blindern, 0316 Oslo, Norway

Institute for Superconducting and Electronic Materials, University of Wollongong,

Northfields Avenue, Wollongong, NSW 2522, Australia and

Centre for Advanced Study at The Norwegian Academy of Science and Letters, Drammensveien 78, 0271 Oslo, Norway

Dendritic flux avalanches is a frequently encountered instability in the vortex matter of type II superconducting films at low temperatures. Previously, linear stability analysis has shown that such avalanches should be nucleated where the flux penetration is deepest. To check this prediction we do numerical simulations on a superconducting rectangle. We find that at low substrate temperature the first avalanches appear exactly in the middle of the long edges, in agreement with the predictions. At higher substrate temperature, where there are no clear predictions from the theory, we find that the location of the first avalanche is decided by fluctuations due to the randomly distributed disorder.

PACS numbers: 74.25.Ha, 68.60.Dv, 74.78.-w

I. INTRODUCTION

Dendritic flux avalanches have been observed in many kinds of type II superconducting films at low temperatures [1]. The origin of the avalanches is a thermomagnetic instability mechanism between the Joule heating created by vortex motion and the reduction of the critical current density as temperature increases [2–4].

When transverse applied field is gradually increased, a critical state is formed from the edges, with almost constant current density, and non-zero magnetic flux density. The flux penetration is gradual and smooth until the conditions for onset of instability is fulfilled. Then, an avalanche is nucleated and large amounts of magnetic flux rushes in from the edges and forms a complex tree-like structure. The onset conditions for such events are determined by a competition between the Joule heating, heat diffusion and heat removal to the substrate [4]. From this theory, it is expected that instabilities are most likely to happen where the electric field is highest and the flux penetration is deepest. Since rectangles in low applied fields experience a flux penetration which is slightly deeper in the middle of the long edges [5], we hence expect the first avalanches to be nucleated there. At higher fields, the flux front straightens out, and it is less clear where the most favorable nucleation location will be.

In this work, we will run numerical simulations of a thermomagnetically unstable superconducting rectangle in applied transverse field. The location of the avalanches will be discussed in context of prediction from linear stability analysis. The simulation method is described in Ref. [6].

II. MODEL

Consider a type II superconducting film subjected to an applied magnetic field transverse to the film plane, ramped at a constant rate \dot{H}_a . The shape of the sample is a rectangle with dimensions $2a \times 2b$.

A thermomagnetic instability is a consequence of the nonlinear material characteristics of type II superconductors, which conventionally is approximated by a power law

$$\mathbf{E} = \frac{\rho_0}{d} \left(\frac{J}{J_c} \right)^{n-1} \mathbf{J}, \quad (1)$$

where \mathbf{E} is electric field, \mathbf{J} is sheet current, $J = |\mathbf{J}|$, ρ_0 is a resistivity constant, d is sample thickness, J_c is critical sheet current, and n is the creep exponent. The temperature dependencies are taken as

$$J_c = J_{c0}(1 - T/T_c), \quad n = n_1/T, \quad (2)$$

where T_c is the critical temperature. The electrodynamics must be supplemented by the heat diffusion equation

$$c\dot{T} = \kappa\nabla^2 T - \frac{h}{d}(T - T_0) + \frac{1}{d}JE, \quad (3)$$

where c is specific heat, κ is thermal conductivity, h is the coefficient for heat removal to the substrate, and T_0 is the substrate temperature.

Eq. (3) must be solved together with Maxwell's equations and the material law, Eq. (1). The description of the simulation method is in Ref. [6] and here only the key ingredients are outlined. The main challenge is to invert the Biot-Savart law in an efficient way. This is done by including also the vacuum outside the sample in the simulation formalism. At the cost of including the extra space, one can use a real space/Fourier space hybrid method with the very attractive performance scaling of $O(N \log N)$, where N is the number of grid points.

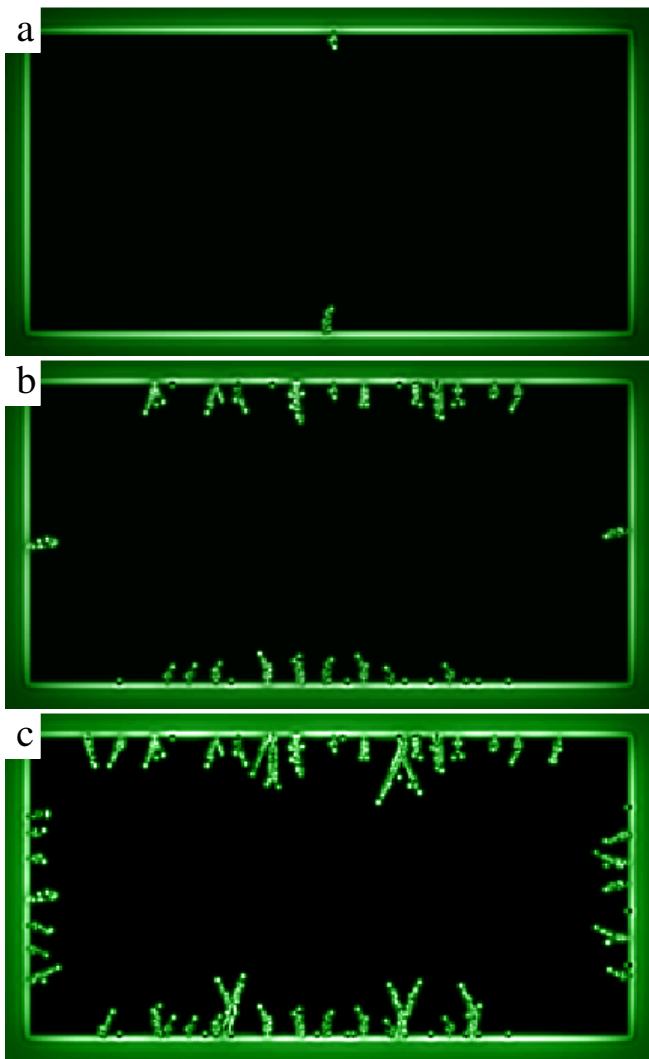


FIG. 1: Distributions of magnetic flux density, B_z , at $H_a/J_{c0} = 0.052$ (a), 0.064 (b), and 0.078 (c). Substrate temperature is $T_0 = 0.17T_c$. The magnetic field is highest at the edges, seen as a white rim, while the black central region is still flux-free, i.e., $B_z = 0$. The avalanches are all small, most of them are fingers, while in (c) some avalanches also have two or three branches.

Quenched disorder is important in order to give realistic nucleation conditions, and it is introduced as a 5% reduction of J_{c0} in randomly selected 5% of the grid points.

The parameters correspond to typical values for MgB₂ films [7]: $T_c = 39$ K, $j_{c0} = 1.2 \times 10^{11}$ A/m², $\rho_n = 7 \mu\Omega\text{cm}$, $\kappa = 170$ W/Km $\times (T/T_c)^3$, $c = 35$ kJ/Km³ $\times (T/T_c)^3$, $h = 200$ kW/Km² $\times (T/T_c)^3$, and $n_1 = 15$. Here ρ_n is normal resistivity, and we have $J_{c0} = dj_{c0}$, and $\rho_0 = \rho_n$. The sample dimensions are $2a = 8$ mm, $2b = 4$ mm, and $d = 0.4 \mu\text{m}$, while the total simulated area is 12×6 mm², where the extra space outside the sample is used to implement the boundary conditions. The total area is discretized on a 768×384 equidistant grid.

III. ANALYTICAL PREDICTION

The linear stability analysis in Ref. [8] determines the condition for instability onset as

$$l^* = \frac{\pi}{2} \sqrt{\frac{d\kappa}{|J'_c|E}} \left(1 - \sqrt{\frac{h}{n|J'_c|E}} \right)^{-1} \quad (4)$$

where l^* is the threshold flux penetration depth, $|J'_c| = J_{c0}T_0/T_c$, and E is the background electric field. For a given E , the sample is unstable when the flux front exceeds l^* , which means that avalanches should appear first where the flux penetration is deepest. In a rectangle, this is in the middle of the two long sides and consequently it is expected that the first avalanches appear there.

IV. SIMULATION RESULTS

The simulations start from initially zero-field cooled state, and the applied field is increased at constant rate, $\mu_0\dot{H}_a = 10$ T/s. The high ramp rate was chosen by performance reasons, since a high ramp rate closes the gap between the velocity of the avalanches and the normal flux penetration. Yet, there is clear separation of time scales, since full penetration is reached in approximately $J_{c0}/\dot{H}_a = 6$ ms, while the duration of the avalanches is less than $0.1 \mu\text{s}$.

Fig. 1 shows the distributions of magnetic flux density transverse to the film plane, B_z , at $H_a/J_{c0} = 0.053$ (a), 0.064 (b), and 0.078 (c). The substrate temperature is $T_0 = 0.17T_c$, and at this low temperature the threshold field for avalanche activity is low, $H_{\text{th}} = 0.052J_{c0}$. Image (a) is just above the threshold, where two small fingers have appeared symmetrically in the middle of the two long edges, just as expected from the theory. In image (b) many more avalanches have come at the long sides, and for the first time there are avalanches appearing at the two short sides, also these in the middle. In image (c) there are even more avalanches and they now cover most of the boundary, except close to the corners. All avalanches are small, and will consequently be seen as small, jumps towards zero in magnetization curves. With increasing field, it seems like a trend of increasing avalanche size.

Fig. 2 shows B_z for a simulation run at a higher substrate temperature, $T_0 = 0.22T_c$. The figure contains just one avalanche, which appeared at $H_{\text{th}} = 0.12J_{c0}$. Both the increased H_{th} and the much larger size of the avalanche is as expected for higher T_0 [8]. Also expected is the complex branching pattern [6]. The location is not entirely symmetric. The reason is that at deeper flux penetrations the flux front straightens out, as seen in regular Bean-state of the upper part of the image. Hence, the location of the avalanche is instead determined by the fluctuations in electric field due to the quenched disorder. The avalanche location is typical for what is seen

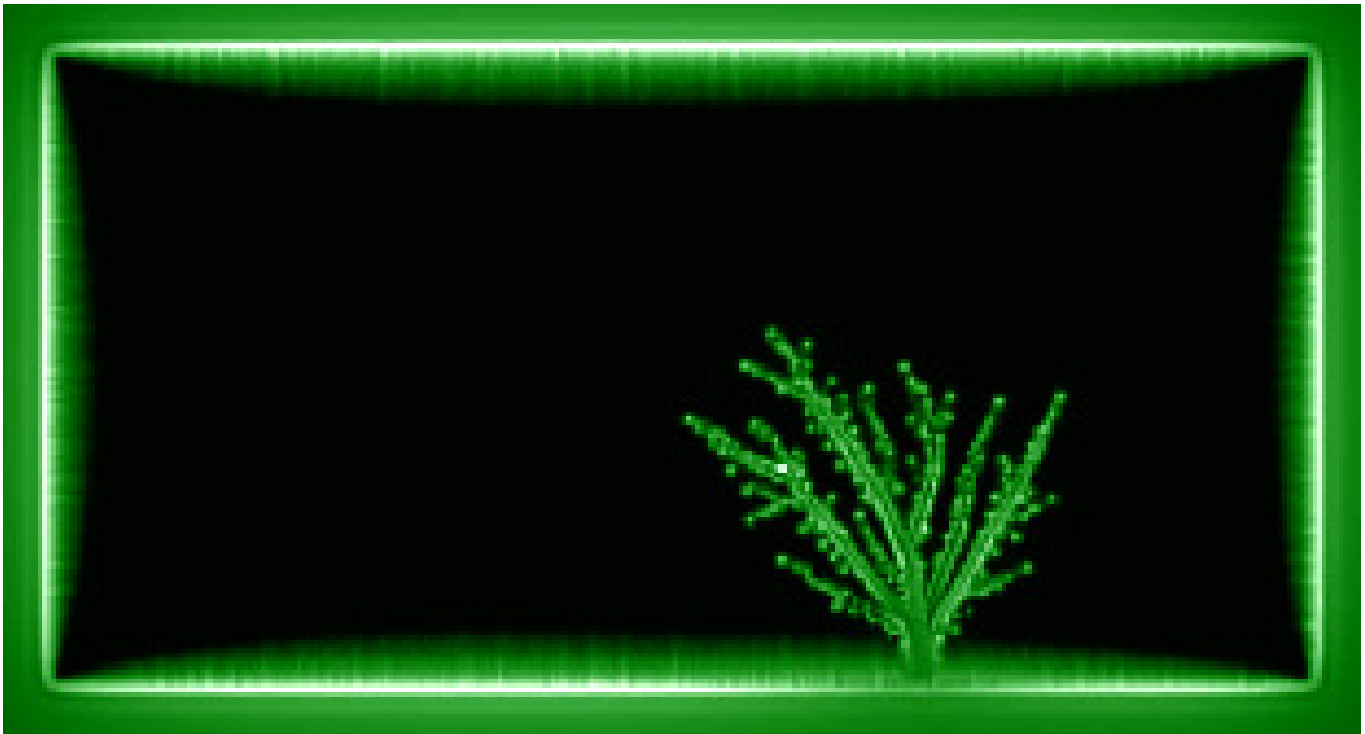


FIG. 2: Distribution of magnetic flux density, B_z , at $H_a/J_{c0} = 0.14$ with substrate temperature $T_0 = 0.22T_c$. Only one dendritic avalanche has been nucleated. Note that the location is not in the middle of the side and the avalanche is larger and have more branches than those at lower T_0 , in Fig. 1.

experimentally, e.g., by magneto-optical images in NbN rectangles [9].

V. CONCLUSIONS

We have simulated dendritic flux avalanches in superconducting films in the shape of a rectangle. The results confirm the prediction from linear stability anal-

ysis that avalanches will first appear in the middle of the long sides, at least for low T_0 . At higher T_0 , the avalanche location was not symmetric. In general, the results regarding avalanche size, threshold field, and time between avalanches follow the typical dependency on T_0 , i.e., that increasing T_0 gives larger H_{th} , larger avalanches, more branches, and longer time between the avalanches. Hence, the simulations of this work also confirms the correctness of the simulation method of Ref. [6].

-
- [1] E. Altshuler, T. H. Johansen, *Rev. Mod. Phys.* 76 (2004) 471.
- [2] R. G. Mints, A. L. Rakhmanov, Critical state stability in type-II superconductors and superconducting-normal-metal composites, *Rev. Mod. Phys.* 53 (1981) 551.
- [3] A. L. Rakhmanov, D. V. Shantsev, Y. M. Galperin, T. H. Johansen, Finger pattern produced by thermomagnetic instability in superconductors, *Phys. Rev. B* 70 (2004) 224502.
- [4] D. V. Denisov, A. L. Rakhmanov, D. V. Shantsev, Y. M. Galperin, T. H. Johansen, Dendritic and uniform flux jumps in superconducting films, *Phys. Rev. B* 73 (1) (2006) 014512.
- [5] E. H. Brandt, Electric field in superconductors with rectangular cross section, *Phys. Rev. B* 52 (21) (1995) 15442.
- [6] J. I. Vestgård, D. V. Shantsev, Y. M. Galperin, T. H. Johansen, Dynamics and morphology of dendritic flux avalanches in superconducting films, *Phys. Rev. B* 84 (2011) 054537.
- [7] M. Schneider, D. Lipp, A. Gladun, P. Zahn, A. Handstein, G. Fuchs, S.-L. Drechsler, M. Richter, K.-H. Müller and H. Rosner, Heat and charge transport properties of MgB₂, *Physica C* 363 (2001) 6.
- [8] D. V. Denisov, D. V. Shantsev, Y. M. Galperin, E.-M. Choi, H.-S. Lee, S.-I. Lee, A. V. Bobyl, P. E. Goa, A. A. F. Olsen, T. H. Johansen, Onset of dendritic flux avalanches in superconducting films, *Phys. Rev. Lett.* 97 (2006) 077002.
- [9] V. V. Yurchenko, D. V. Shantsev, T. H. Johansen, M. R. Nevala, I. J. Maasilta, K. Senapati, R. C. Budhani, Reentrant stability of superconducting films and the vanishing of dendritic flux instability, *Phys. Rev. B* 76 (9) (2007) 092504.